HAL
open science

# Time-resolved electric field measurements in nanosecond surface dielectric discharge. Comparison of different polarities. Ignition of combustible mixtures by surface discharge in rapid compression machine (AIAA 2013-1053)

S.A. Stepanyan, M.A. Boumehdi, G. Vanhove, Svetlana Starikovskaia

## To cite this version:

S.A. Stepanyan, M.A. Boumehdi, G. Vanhove, Svetlana Starikovskaia. Time-resolved electric field measurements in nanosecond surface dielectric discharge. Comparison of different polarities. Ignition of combustible mixtures by surface discharge in rapid compression machine (AIAA 2013-1053). 51st AIAA Aerospace Sciences Meeting, Jan 2013, Grapevine, Texas, United States. hal-02588012

**HAL Id: hal-02588012**

**https://hal.science/hal-02588012v1**

Submitted on 21 Sep 2020

**HAL** is a multi-disciplinary open access archive for the deposit and dissemination of scientific research documents, whether they are published or not. The documents may come from teaching and research institutions in France or abroad, or from public or private research centers.

L'archive ouverte pluridisciplinaire **HAL**, est destinée au dépôt et à la diffusion de documents scientifiques de niveau recherche, publiés ou non, émanant des établissements d'enseignement et de recherche français ou étrangers, des laboratoires publics ou privés.

# Time–resolved electric field measurements in nanosecond surface dielectric discharge. Comparison of different polarities. Ignition of combustible mixtures by surface discharge in a rapid compression machine.

S.A. Stepanyan, * M. A. Boumehdi, † G. Vanhove, ‡ S.M. Starikovskaia, §

*Laboratory for Plasma Physics, Ecole Polytechnique, Route de Saclay, 91128, Palaiseau Cedex, France*

*PC2A Lille University of Science and Technology, 59655, Villeneuve d'Ascq, France*

**Surface nanosecond dielectric barrier discharge has been studied in air and at pressures ranging from 1 to 5 bar, with a coaxial geometry of the electrodes for positive and negative polarities of the high-voltage pulses. Pulses of a 24–55 kV amplitude on the electrode, positive or negative polarity, 20 ns duration, 0.5 ns rise time and 10 Hz repetitive frequency were used to initiate the discharge. ICCD images of the discharge development have been taken with a 2 ns gate. In the case of discharges in nitrogen, the emissions of molecular bands of the first negative and second positive systems of molecular nitrogen have been measured, and the dependence of their ratio versus pressure and distance from the high-voltage electrode has been analyzed. A comparison of the discharge development has been made in the case of negative and positive polarities at the high-voltage electrode.**

**Ignition delay times under the action of a high-voltage nanosecond discharge have been studied and compared with autoignition delays in a rapid compression machine (RCM). The nanosecond Surface Dielectric Barrier Discharge (SDBD) was initiated in a quasi-uniform radial geometry in the proximity of the end plate of the combustion chamber of the RCM. Experiments were performed for methane and n-butane containing mixtures diluted by Ar or $N_2$ for temperatures and pressures at the end of compression respectively ranging from 650 to 1000 K and 6 to 16 bar. A significant decrease of the ignition delay time is observed, when compared to autoignition experiments. The possibility to ignite lean mixtures is demonstrated. Preliminary experiments in the region of negative temperature coefficient for stoichiometric n–butane:oxygen mixture diluted with argon, are performed. The threshold voltage for plasma ignition, over which the ignition delay is decreased, is studied for different mixtures.**

## I. Introduction

Plasma assisted ignition and combustion have been intensively studied for the last 10–15 years. Recent review papers[1–4] analyze original publications and prove that low-temperature non equilibrium plasmas can be efficient tools for the initiation of combustion processes (PAI, or plasma-assisted ignition) in a wide range of initial pressure conditions, as well as for the sustainment of combustion in the case of lean mixtures (PAC, or plasma-assisted combustion).

Over the last decade, significant progress has been made in understanding the mechanisms of plasma-chemistry interactions, energy branching for discharge plasmas of combustible gas mixtures, and non-equilibrium initiation of combustion. The analysis of the main factors responsible for the PAI/PAC[1–4]

*PhD Student, Laboratory for Plasma Physics, Ecole Polytechnique, Palaiseau, France

†PhD Student, Laboratory of Physics of Physico–Chemical Processes in Combustion and in Atmosphere, Lille University, France

‡Senior Researcher, Laboratory of Physics of Physico–Chemical Processes in Combustion and in Atmosphere, Lille University, France

§Leading Researcher, Laboratory for Plasma Physics, Ecole Polytechnique, Palaiseau, France

shows that at high electric fields, in spatially uniform configuration, at relatively high initial temperatures, and at the vicinity of the ignition threshold, the main mechanism of initiation or support of the combustion process is the dissociation of molecules via electronically excited states and the production of radicals. These radicals are responsible for partial fuel conversion through similar chemical reactions as those observed in the case of ignition processes.

The idea to combine the "traditional" shock tube technique used for measurements of autoignition delay times with the high-voltage technique used for nanosecond discharges comes from the Physics of Nonequilibrium Systems Laboratory at the Moscow Institute of Physics and Technology, and has been developed intensively over the period 1996-2008. After preliminary calculations,[5] the experimental setup combining a shock tube with high-voltage spatially uniform nanosecond discharges[6] quantitatively demonstrated a principal benefit of low temperature plasma application for ignition: for $H_2/O_2$ stoichiometric mixture, diluted by Ar with a molar fraction of 80 %, plasma-assisted ignition occurred at temperatures 600 K lower than autoignition. If to assume that all the discharge energy (about 50 mJ/cm$^3$) goes to gas heating (so-called "equilibrium approximation"), and to calculate the autoignition delay for the obtained temperature, this shift will be equal to 20 K instead of 600 K. So, the nonequilibrium nature of the observed decrease of the ignition delay time was clearly demonstrated. A series of papers combining experimental measurements and calculations have been published,[7–10] confirming this result and providing a broad set of data for temperatures close to the ignition threshold (880-1970 K) and pressures between 0.2 and 2.2 bar. A few evidences of high–pressure ignition by nanosecond discharges are presented in the literature.[11–14]

Recently, it was suggested[15] to use a "two-dimentional" dielectric surface barrier nanosecond discharge in combination with a rapid compression machine (RCM) to initiate the ignition at high pressures and lower temperatures. This type of discharge was proposed[16] in linear electrode configuration and used for aerodynamic actuators.[17,18] In our idea, the radial geometry of the discharge[15] offers the possibility to decrease the hydrodynamic effects caused by the simultaneous (within 0.2 ns) start of streamer channels from the high-voltage electrode.

Rapid Compression Machines are widely used to study ignition phenomena in physical conditions close to those of engines.[19] They can simulate a single compression stroke and bring a gas mixture to temperature and pressure conditions that are difficult to reach with other apparatuses such as shock tubes, i.e. pressures from 5 to 40 bar and temperatures in the range 600–1000 K. They allow the measurement of ignition delay times in a well–controlled homogeneous environment. Typical reaction times are from one to hundreds of milliseconds, depending on the duration of the compression stroke and the characterization of the reacting mixture after the compression. Given that the heat losses are accurately reproduced,[20,21] the measured autoignition delays can be reasonably well reproduced using 0D models.[22] The application of pulsed plasma in an RCM environment would therefore significantly broaden the current range of investigated parameters for plasma assisted ignition and could extend the knowledge of its mechanisms and efficiency at low temperatures and high pressures.

The main difference between "traditional" spark plug ignition (which is, generally speaking, an equilibrium pulsed plasma, where the temperature of the gases is high, i.e. a few thousand K, and equal to the temperature of electrons) and the ignition by nonequilibrium plasma (which is traditionally called "plasma-assisted ignition") is that, instead of direct and local heating of a gas under study, a certain density of ions/radicals/excited species are produced locally or uniformly in the streamer volume. This causes fast heating due to recombination and relaxation, but also can initiate chemical chain branching.

The first known RCM–nanosecond plasma experiences have been published by.[23] Three electrode geometries were used for the pulsed discharge: localized nanosecond spark, surface dielectric barrier discharge (SDBD) with a pin–like electrode, and a streamer corona. The discharge was initiated by a 40 kV voltage pulse in the cable, the amplitude on the electrode being 80 kV; the energy input was approximately 200-300 mJ in the spark configuration and less than 50 mJ in the case of the DBD discharge. Ignition of combustible mixtures by the discharge was studied, the discharge occurring during and after compression. The authors demonstrated a decrease of the ignition delay time from hundreds to tens of milliseconds for propane: air stoichiometric and lean (ER=0.4) mixtures in the pressure range 17–40 bar and temperatures 700–1000 K. The observed ignition delay time depends upon the type of the discharge, and the instant of the discharge initiation. Although clearly demonstrating the effect, paper[23] does not develop the study of the discharge itself and deals with a constant voltage.

The aim of the present work is to perform an initial series of RCM experiments in well–controlled conditions of diluted mixtures, comparing data for autoignition and plasma–assisted ignition, if available,

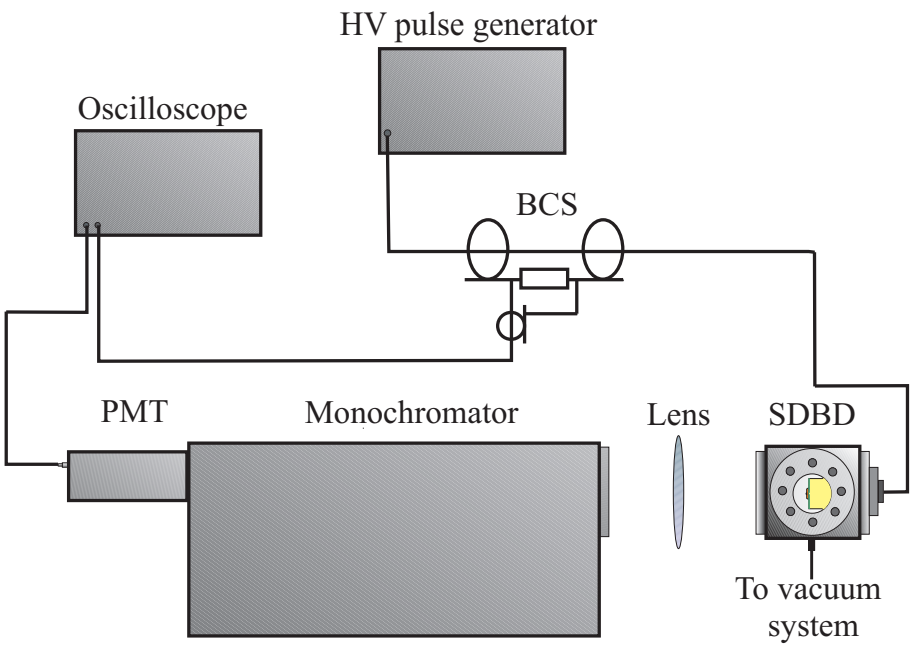


**Figure 1. scheme for electric field measurements.**

and analyzing the behavior of pressure traces as a function of the parameters of the discharge (voltage and polarity) and of the investigated mixture (equivalence ratio, choice of the fuel, pressure and temperature).

## II. Experimental setup

### A. Discharge experiments. ICCD imaging and electric field measurements

A general scheme of the experimental setup is presented in figure 1. The high pressure discharge cell is made of stainless steel and has three optical quartz windows, with a thickness of 15 mm and a diameter of 50 mm. The discharge chamber allows pumping down to $1.6{\cdot}10^{-2}$ Torr before it is filled by the investigated gas mixture. Two pressure gauges are used to measure the pressure: Pfeiffer capacitive vacuum gauge for the pressures lower than 10 Torr and SCM capacitive gauge for the pressures higher than 1 bar. The chamber has been tested up to a pressure P=8 bar, and the experiments have been carried out for a pressure range of 1-5 bar. Synthetic air (80% $N_2$, 20% $O_2$, Air Liquide, impurities did not exceed 3 ppm) has been used for the experiments.

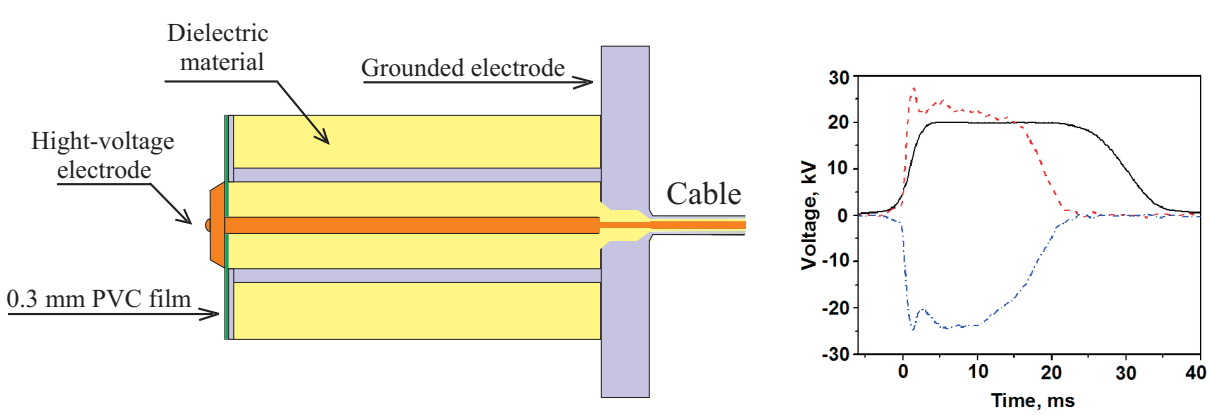


**Figure 2. electrode system and applied pulses.**

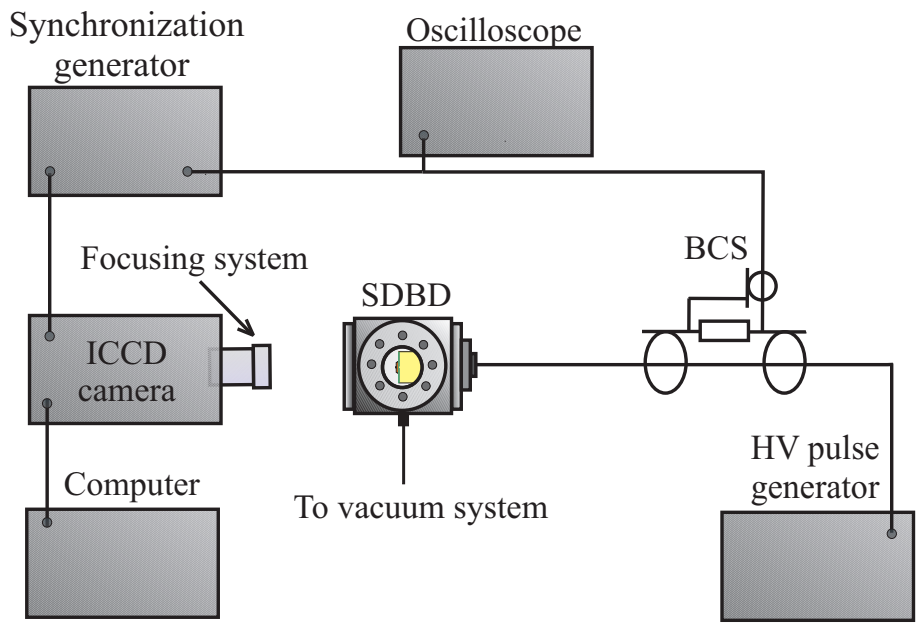


**Figure 3. Scheme of ICCD imaging.BCS–back current shunt, HV–high voltage.**

A coaxial electrode system,[15] schematically represented by figure 2, has been developed to obtain a quasi-uniform discharge that propagates along the surface in a radially symmetrical geometry. The central coaxial high voltage (HV) electrode is connected to a copper disk, 2 mm in thickness and 20 mm in diameter. The low voltage electrode is made of aluminum. The inner diameter of the low voltage electrode is equal to the outer diameter of the HV electrode, and the outer diameter is equal to 46 mm. A dielectric layer of PVC is located between the electrodes. The discharge is initiated from the edge of the disk and propagates above the surface of PVC layer.

During the following experiments, the SDBD electrode system was installed into one of the ports of the high pressure discharge cell, so that one optical window was situated opposite to the electrode system and the others allowed to observe the discharge from the side. The high voltage electrode was connected to the high-voltage generator via a 30 m coaxial 50 Ω cable. The FID high–voltage (HV) pulse generator FPG20–03NM used in experiments provided the following parameters: 0.5 ns pulse front rise time, 20 ns pulse duration and ± (12–30) kV voltage range in the cable (see fig. 2). All discharge SDBD experiments presented in this paper were performed at a frequency of 10 Hz, and without a gas flow.

Two calibrated back current shunts (BCS) were installed into the cable: one (BCS1) in the middle of the cable and another one (BCS2) at 1 m from the HV generator. BCS1 was used to calculate the energy deposited into the discharge, and BSC2 was used to synchronize the ICCD camera with the discharge. The signals from the BCS were registered by a LeCroy WaveRunner 600 MHz oscilloscope.

To study the spatial structure and the development of the surface discharge, a 2D map of emission integrated over the wavelength range 300-800 nm was recorded with an (ANDOR) ICCD camera.

The camera gate was equal to 2 ns. In the case of a nanosecond SDBD, the main emission in this spectral range is due to transitions of the second positive system of molecular nitrogen. For air, the quenching time is determined by the collision of excited nitrogen molecules with molecular oxygen, the rate constant being equal to $k$=2.7 $\cdot$ $10^{-10}$ $cm^3s^{-1}$, data from.[24] The efficient life time of $N_2(C^3\Pi_u)$ is 0.7 ns at the atmospheric pressure and 0.14 ns at $P$ = 5 atm, thus ICCD imaging adequately reflects the spatial structure of the discharge, and the resolution is limited by the camera gate. The scheme of the ICCD synchronization is given by figure 3. ICCD camera was triggered by the BCS signal through the synchronization generator with a tunable delay, and the ICCD images corresponding to different instants from the discharge initiation were obtained by varying the camera gate delay.

To analyze the electric field behavior, space– and time–resolved emission of 0–0 vibrational transitions of the second positive (337.1 nm) system of molecular nitrogen and of the first negative (391.4 nm) system of molecular nitrogen ion was measured. The details of the procedure can be found elsewhere,[25–27] and

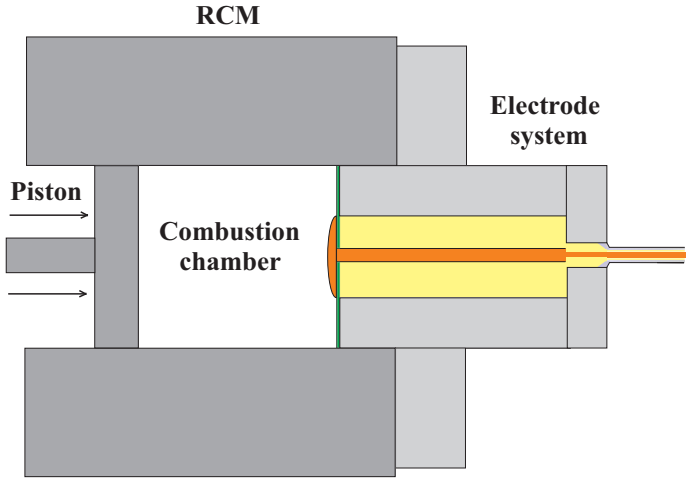


**Figure 4. scheme of RCM combustion chamber with installed electrode system.**

the procedure was similar to that used in.[27] The emission from SDBD was focused onto the input slit of an Andor SR–500i monochromator (1200 l/mm grating, 1.65 nm/mm dispersion). Hamamatsu H6610 Photomultiplier tube (PMT) was connected to the output of the monochromator. The signal from the PMT was recorded by the oscilloscope. A Broad–band glass filter was used to reduce the intensity of emission in the UV spectrum range (at the wavelength of 337.1 nm) to perform the measurements of both molecular bands at similar PMT voltages. The slits of the monochromator were adjusted so that the only molecular band of interest was monitored during the experiments: the entrance slit of the monochromator was set to the value of 1.84 mm for the recording of the emission of the second positive system of $N_2$ and 1.05 mm for the measurements of the emission of the first negative system of $N_2$.

Four concentric plastic diaphragms of different diameters installed 3 mm above the dielectric layer coaxially to the electrode system were used to select the radiation from different regions of the discharge. The difference in external and internal diameter of each diaphragm was 2 mm, and the diaphragms were installed at the distances 0, 3, 6, and 9 mm from the 20 mm diameter high-voltage electrode.

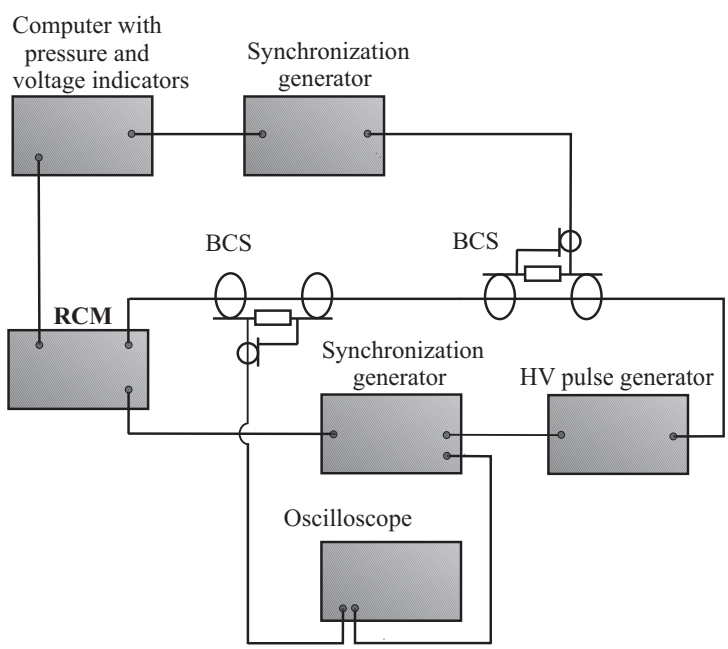


**Figure 5. scheme of synchronization for the plasma assisted experiments on RCM.**

### B. Combustion experiments. Rapid compression machine.

An electrode system, very similar to the one described above (see fig. 4), was mounted on the RCM designed at PC2A, University of Lille, to initiate the high-voltage nanosecond discharge near Top Dead Centre (TDC). The RCM combustion chamber is a cylinder which diameter is 50 mm and height at TDC is 16 mm. it is equipped with a creviced piston following the recommendations of.[28] The reaction chamber can be heated uniformly to selected temperatures, and is equipped with a Kistler 601 A piezoelectric pressure transducer, a sampling port and two optical windows. The analog signals are acquired with a National Instruments card linked to a computer, with a time step of 40 $\mu$s.

The investigated mixtures were prepared following the partial pressures method using a glass facility and gases provided by Air Liquide. The purities of the gases were: Methane 99.95%, n–butane 99.5%, oxygen 99.995%, nitrogen 99.996%, Argon 99.9990%.

The electrode system was substituted to the end plate of the RCM. The electrode system was very similar to the system used in SDBD experiments (compare to fig. 2) with the only difference being that the high-voltage electrode was made as a segment of a sphere, and its height did not exceed 1 mm.

The synchronization setup presented in figure 5 was used to initiate the discharge at a given instant close to TDC. A TTL signal from the Acquisition/Command NI card was used to initiate the compression. The start of the piston being recorded by an optoelectrical element, the high–voltage FPG20–03NM generator was triggered after a given delay corresponding to the compression time. As the high-voltage signal propagated through the cable, the back current shunt was used to mark the discharge initiation together with the pressure trace. Two synchronization generators, for preliminary and fine adjustment, were used to fix the delay between the compression beginning and the initiation of the discharge. The delay between TDC and the discharge initiation was fixed to 2–3 ms, that is was also much shorter than the autoignition delay time (60 ms and longer) and shorter that typical time of heat losses.

To discriminate between the chemical processes involved in the initiation of the combustion and the consequent propagation of the flame inside the high pressure environment, the ignition time was measured using the tangent method described in figure 11. The ignition delay in the case of autoignition is defined as the time between TDC and the ignition time. In the case of plasma–assisted ignition, it is defined as the difference between the discharge and the ignition time.

## III. Experimental results

This chapter consists of two parts which describe the obtained experimental results. The first part describes the electric field measurements in nanosecond SDBD initiated in synthetic air at different pressures and voltages. The measurements include the electric field evolution and its spatial distribution. The first part also includes the results of ICCD imaging of SDBD. The second part represents part represents the experiments on plasma assisted combustion.

### A. Electric field measurements and ICCD imaging

Figure 6 represents the dependence of the electric field evolution near the edge of HV electrode at different pressures and different pulse polarities. The experiments were performed is dry air and the voltage amplitude of the pulses applied in experiments represented by black solid lines was 12 kV which corresponds to 24 kV on HV electrode. Rise front time was 0.5 ns, pulse duration was 20 ns. Dashed red lines in the fig. 6 and 7 represent the experiments with +20 kV on HV electrode (front rise time 2 ns, pulse duration 30 ns) at 10 Hz frequency. Typically the electric field reaches its maximum and then it decreases to its minimum and than rises again. It is clearly seen that the maximal electric field is higher for positive polarity pulses. It must be also noted the maximal electric field is higher for lower pressures at the range (1–3) atm and approximately the same at the range (3–5) atm. The same is valid for minimal pressure for both polarities.

Figures 7 and 8 represent the electric field evolution at 3 mm and 6 mm from HV electrode for different pressures and pulse polarities. Comparison of fig. 6 and 7 shows that the electric field (both maximal and minimal) for positive polarity pulses is higher at 3 mm from HV electrode than at 0 mm. At the same time the electric field (neither maximal nor negative) corresponding to the negative polarity pulses at 1 atm is lower at 3 mm from HV electrode than at 0 mm from HV electrode. But at 2 atm the situation is opposite, i.e. the electric field is higher at 3 mm from HV electrode than at 0 mm.

Figure 8 demonstrates that the highest values of the electric field occur near the edge of grounded

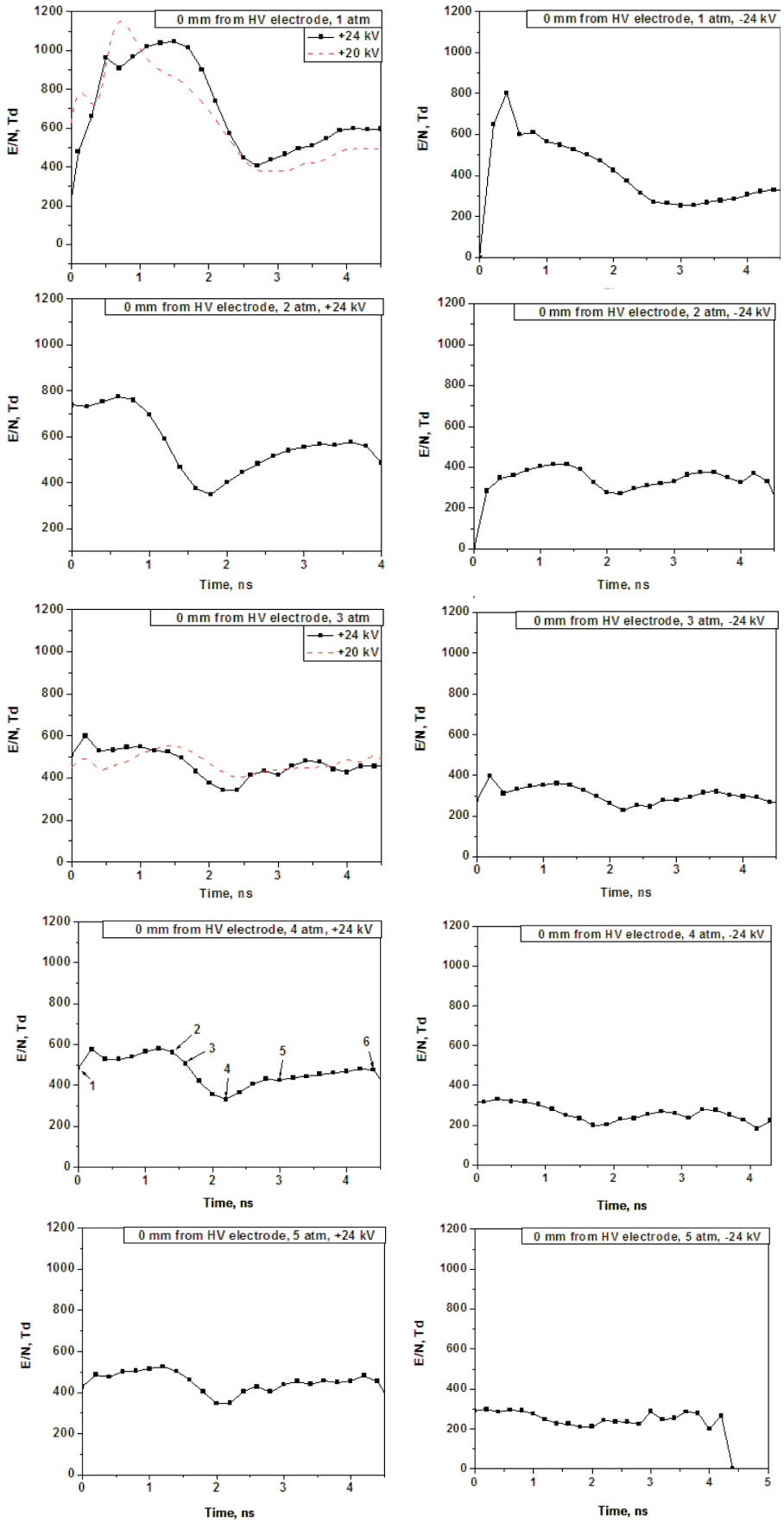


**Figure 6. Comparison of the electric field evolution near the HV electrode for the different pressures and polarities. Synthetic air.**

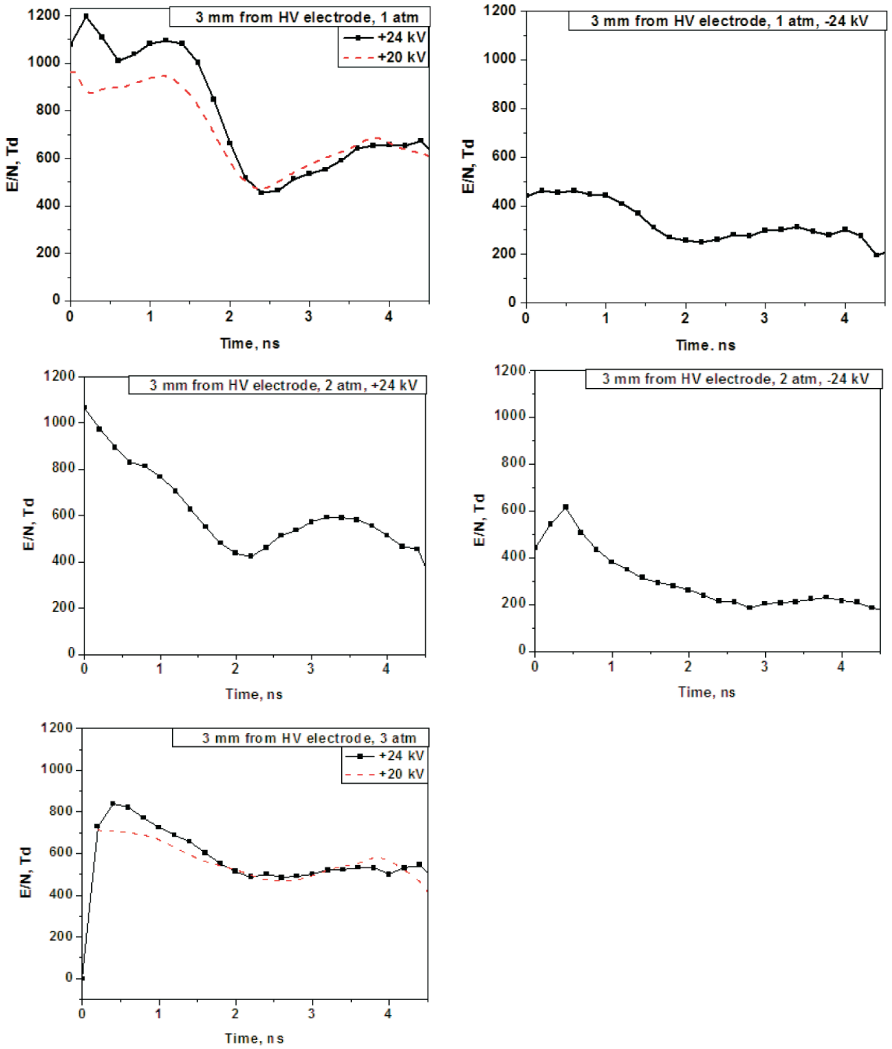


**Figure 7. Comparison of the electric field evolution at 3 mm from HV electrode for the different pressures and polarities. Synthetic air.**

electrode, i.e. at longer distance from HV electrode. These results confirm that the both maximal and minimal electric fields are higher for positive polarity pulses. It should be also noticed that the electric field at 6 mm from HV electrode for positive polarity at 2 atm is higher than for 1 atm. The dependencies of the electric field at 6 mm for higher pressures are not presented because of low signal of the emission intensity at 391.4 nm.

Regarding the results presented above it is necessary to keep in mind that the method used to obtain the electric field by emission ratio R391/337 implies the uniformity of the plasma. Some works[29,30] predict for positive polarity the gap between the streamer and the surface above which it propagates. If it is feasible at the conditions concerned above then the following situation is possible: instead of the emission at 337.1 and 391.4 nm from uniform plasma it was measured the composition of the radiation from the plasma and from the "gap". The electron density in a gap is significantly lower than in a plasma, but at the same time the electric field is significantly higher in a "gap" which may be the reason of the same order (or even higher) of the emission intensity in a "gap" and in a plasma at 337.1 and 391.4 nm.

To follow the discharge transformation with pressure and/or voltage amplitude, ICCD imaging in 250-800 nm spectral range was made for a negative polarity pulse, for synthetic air (24–55 kV amplitude on the electrode, 1–5 atm) and for Ar (24 kV amplitude, 3 and 5 atm pressure). The ICCD camera gate was 2 ns, and the delay between the beginning of the discharge and the ICCD gate was shifted to obtain a time history of the discharge development.

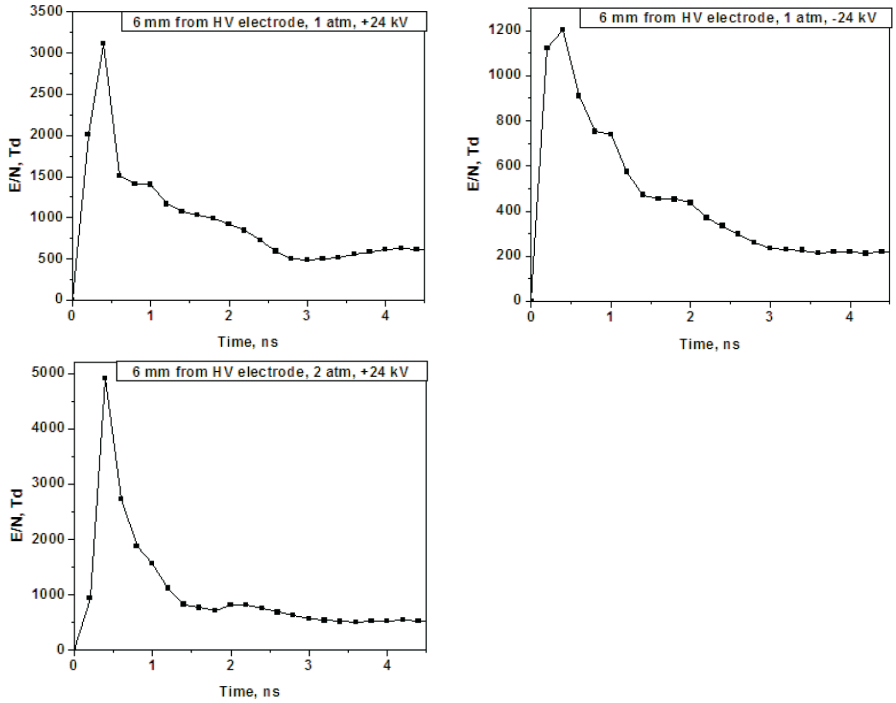


**Figure 8. Comparison of the electric field evolution at 6 mm from HV electrode for the different pressures and polarities. Synthetic air.**

For argon, the emission lasted at least hundreds of nanoseconds; additional spectral analysis is needed to identify the origin of the emission. For air, short life–time emission of the second positive system of molecular nitrogen was observed; the emission pulses behavior with time corresponded to the pulses of current.

Both for air and for nitrogen, the discharge develops in a radial direction, from the high–voltage electrode along the dielectric (PVC) surface. The thickness of the discharge is not higher than a few millimeters.

Typical ICCD images for the discharge in air are given by figure 9. Black circle in the center of the image

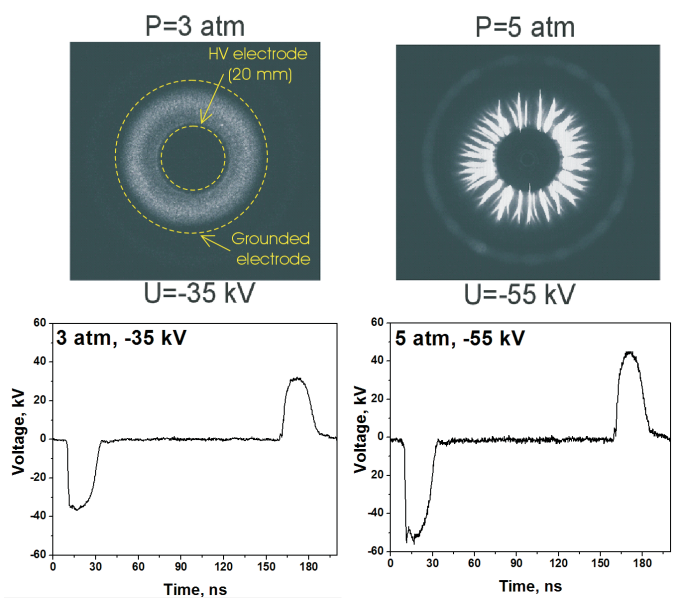


**Figure 9. Diffusive and filamentous modes. Back current shunt oscillograms. Synthetic air.**

corresponds to the high–voltage electrode 20 mm in diameter. Two forms of the discharge were observed in air: at low pressures and low voltages discharge developed as a quasi–uniform structure with a central symmetry relative to the center of the electrode (photo on the right). With pressure/voltage increase, a bright structure has been observed (photo on the left). To check the nature of the discharge, the back current shunt signals were analyzed. It follows (and it is illustrated by oscillograms given by figure 9) that there is no electrical gap closing for any of the considered discharge form, so both discharge forms correspond to low–current streamer regime. It is also important to mote that, at high pressures and high amplitudes, the channels are bright starting from the first nanoseconds of their development from the high–voltage electrode, when the gap is definitely not closed. The threshold for discharge transition to a high emission intensity form depends upon pressure: at 3 atm the transition is observed at –53 kV, at 5 atm it is observed at about –40 kV.

For Ar, experiments at 3 and 5 atm at –24 kV of the voltage amplitude were performed. The discharge in Ar is brighter than discharge in air; the structure of the discharge and peculiarities of the development are quite similar.

## B. Plasma assisted combustion experiments

Gas mixtures, pressures and temperatures checked in RCM experiments, are given by 1.

**Table 1. Mixtures and gas parameters used in RCM experiments**

| N | Mixture | $T_c$, K | $P_{TDC}$, atm |
|---|---|---|---|
| 1 | $CH_4$:$O_2$:Ar, $\phi = 0.3$, 76% of Ar | 962 | 16 |
| 2 | $CH_4$:$O_2$:Ar, $\phi = 0.5$, 76% of Ar | 942 | 16 |
| 3 | n–$C_4H_{10}$:$O_2$:$N_2$, $\phi = 1$, 76% of $N_2$ | 665—720 | 7.5 |
| 4 | n–$C_4H_{10}$:$O_2$:Ar, $\phi = 1$, 76% of Ar | 815—895 | 8.5 |
| 5 | n–$C_4H_{10}$:$O_2$:$N_2$:Ar, $\phi = 1$, 38% of $N_2$, 38% of Ar | 710 | 7.9 |

A typical difference between autoignition and plasma assisted ignition pressure-time profiles is shown in fig. 10. To help discriminate the compression phase from the ignition, the time between TDC and the discharge initiation in figure 10(b) is artificially made longer, about 10 ms. Usually for all the experiments this delay was kept within 2–3 ms, to minimize the heat losses in the combustion chamber. It is clearly seen that for plasma assisted ignition, the discharge significantly decreases the ignition delay time, from tens

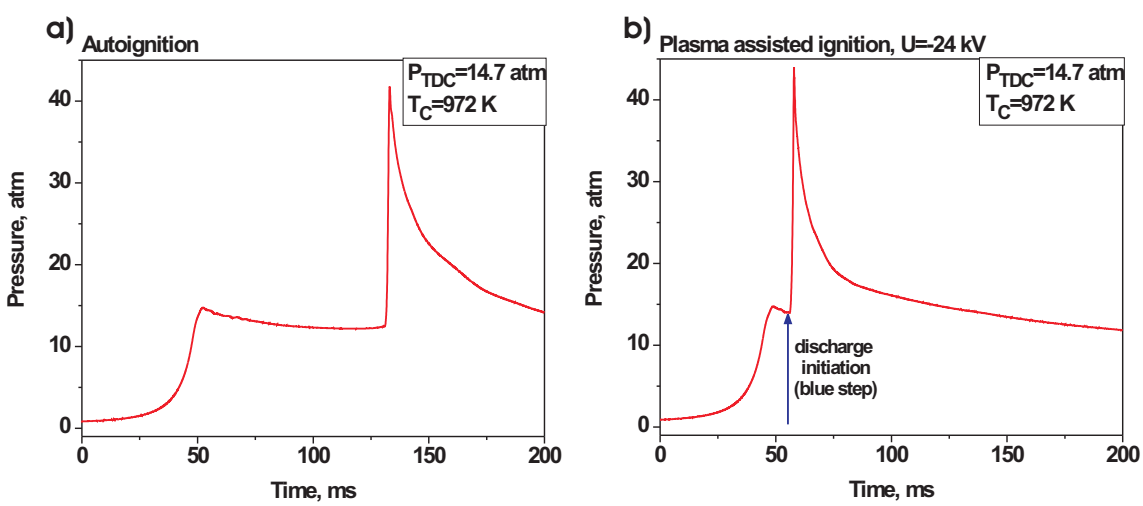


**Figure 10. Comparison of the a) autoignition and b) plasma assisted ignition. Methane/oxygen stoichiometric mixture diluted by 71 % of argon.**

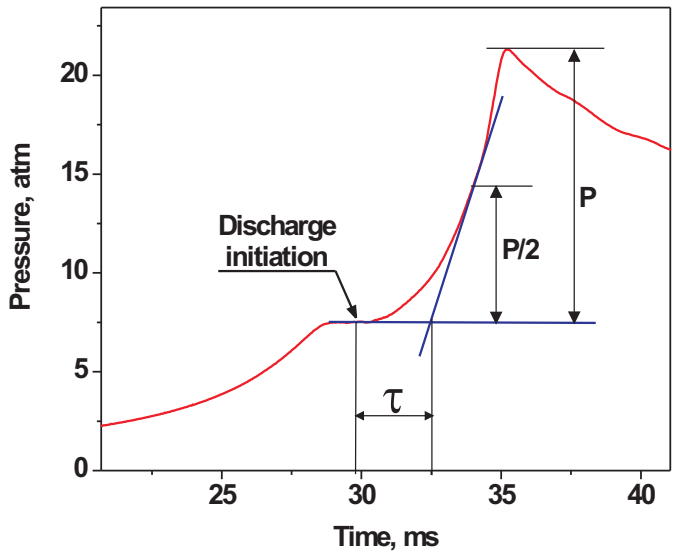


**Figure 11. Definition of the induction time.**

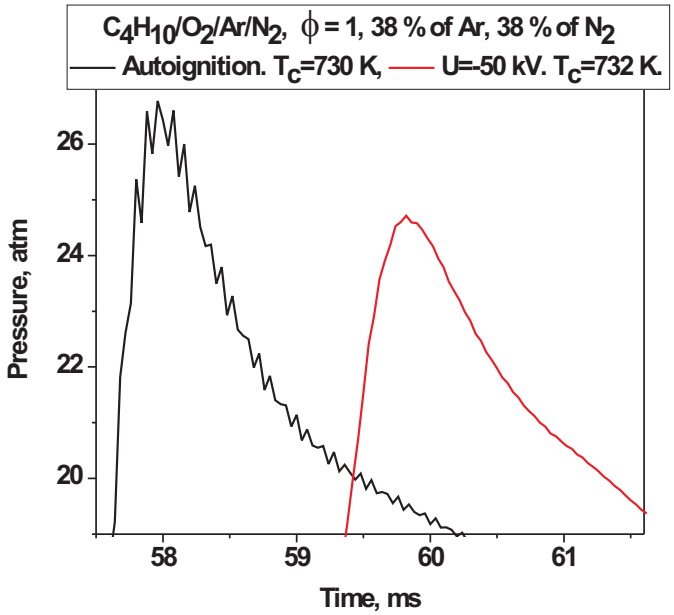


**Figure 12. Comparison of the autoignition (black) and plasma assisted ignition (red) for n–butane/oxygen stoichiometric mixture diluted by 38 % of Ar and 38 % of $N_2$: comparison of pressure profiles near the maximal pressures.**

of milliseconds to milliseconds. For the combustion initiation by similar sliding DBD discharge at ambient temperature, it was suggested in[15] that the main action of plasma is due to creation, at the perimeter of a high-voltage electrode, a few tens of "hot spots" with elevated density of radicals produced when streamers start from the electrode, and increased gas temperature, due to relaxation, within a microsecond time scale, of the energy stored in electronic excitation of atoms and molecules. For considered RCM experiments,

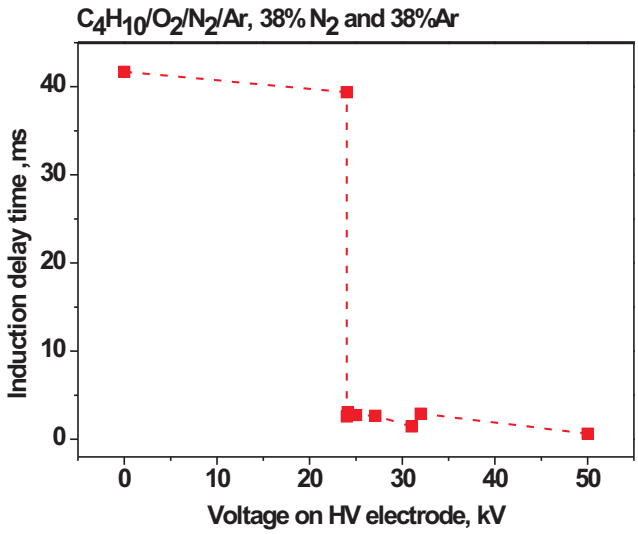


**Figure 13. Dependence of the induction time on voltage for n–butane/oxygen stoichiometric mixture diluted by 38 % of Ar and 38 % of $N_2$. Negative polarity pulses.**

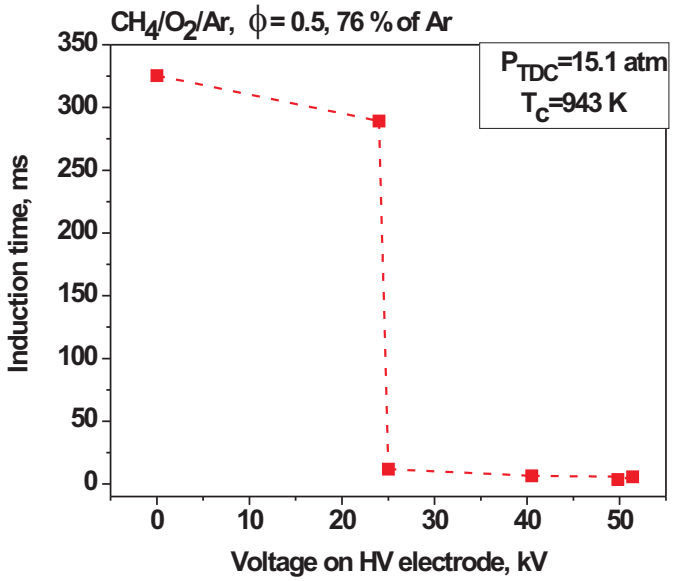


**Figure 14. Dependence of the induction time on voltage. Methane/oxygen lean mixture ($\phi$=0.5) diluted by 76 % of Ar. Negative polarity pulses.**

it is still unclear if the observed decrease of ignition delay time is due to multi-point ignition at the edge of the high-voltage electrode (caused by both the dissociation and temperature increase) and the following flame propagation or to a more volumetric ignition initiated by preliminary quasi-uniform dissociation in the vicinity of the end plate; additional experiments are planned for the visualization of the subsequent propagation of the combustion inside the combustion chamber.

One of the noticeable results is that, in stoichiometric mixtures, when the discharge is induced, the rate of pressure increase relative to ignition can be smaller than in the case of autoignition. In some cases, this

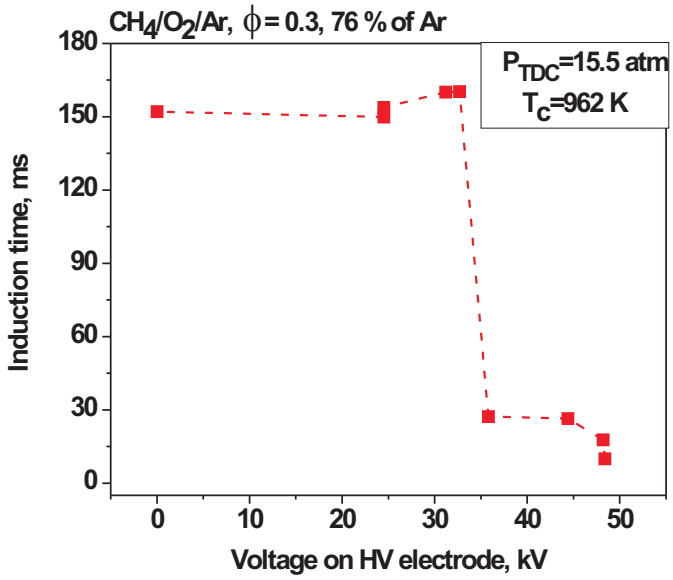


**Figure 15. Dependence of the induction time on voltage. Methane/oxygen lean mixture ($\phi$=0.3) diluted by 76 % of Ar. Negative polarity pulses.**

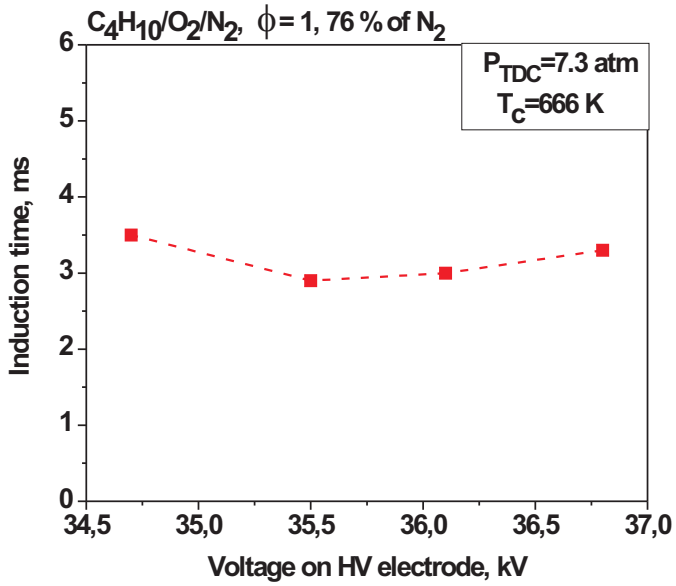


**Figure 16. Dependence of the induction time on voltage for n–butane/oxygen stoichiometric mixture diluted by 76 % of $N_2$. Negative polarity pulses.**

can result in a reduction of knocking, as for example in the case of stoichiometric n-butane/oxygen mixtures diluted by an equimolar mixture of nitrogen and argon. This is illustrated in figure 12. The pressure curve, in the autoignition case, shows high frequency oscillations that are typical of mild knocking, whereas, in the plasma assisted ignition case, those cannot be seen. This has been observed consistently in these experimental conditions.

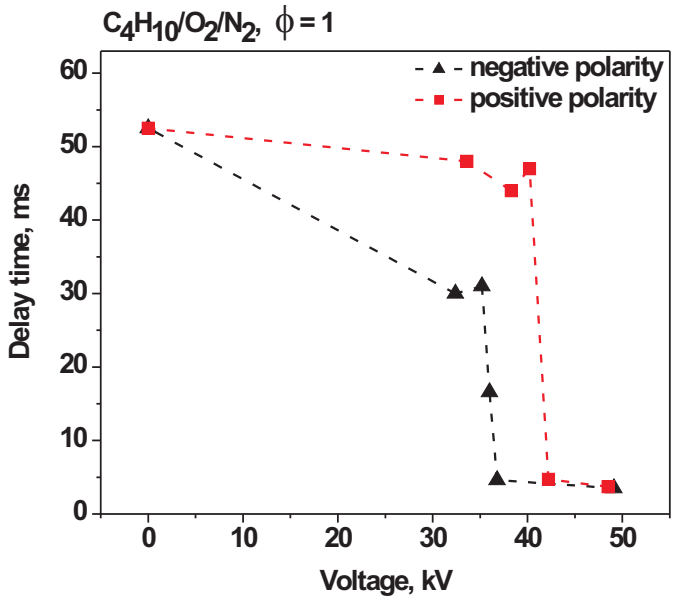


**Figure 17. Dependence of the induction time on voltage. Comparison of negative and positive polarity pulses for n–butane/oxygen stoichiometric mixture diluted by 76 % of $N_2$.**

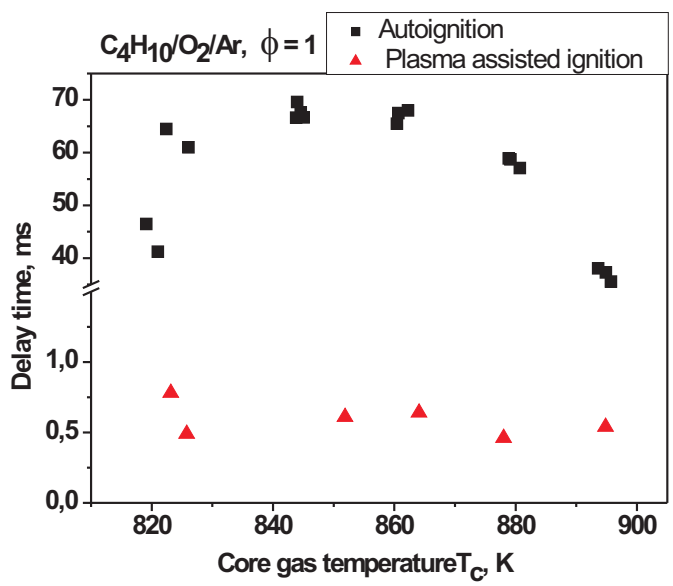


**Figure 18. Comparison of autoignition and plasma assisted ignition in the NTC region for n–butane/oxygen stoichiometric mixture diluted by 76 % of Ar.**

Figures 13-17 summarize the experimental data on the evolution of the ignition delay as a function of the voltage on the electrode. The experiments have been done for a negative polarity of the high voltage pulse. It should be noted here, that, strictly speaking, the voltage amplitude itself cannot be considered as a parameter for comparison and physical conclusion about the action of the discharge. Experiments in air (see

for the details section "Electric field measurements and ICCD imaging" prove that discharge morphology can be changed significantly with voltage amplitude. It is well–known that additions of combustible gases, like methane of acetylene, can have a significant effect on the morphology of the discharge, decreasing its spatial uniformity.[31] So, an additional study of the discharge geometry is necessary to understand the physics of the threshold observed. For the moment, we consider the discharge as quasi-uniform referring to the relatively low voltages of the threshold (figs. 14–17) and ICCD imaging in air and argon. As it is seen from figures 13-17, for a voltage superior to a given value –later referred to as threshold voltage– the ignition delay time drops sharply, from a value close to the autoignition case to a much shorter value.

It is worth noting that changing the polarity of the high-voltage pulse has a significant effect on the threshold voltage, as can be seen in fig. 17. In the case of a n-butane/$O_2$/$N_2$ mixtures, the threshold voltage is higher for a positive polarity than for a negative polarity of the pulse. This fact needs additional experimental and numerical analysis of the discharge initiation, propagation, and influence on the investigated gas mixture to explain the difference between the two observed polarities.

Figure 18 represents the dependence of the induction delay time on the core gas temperature $T_c$, in the case of a Negative Temperature Coefficient (NTC). In this situation, complex thermokinetic interactions cause an increase in the ignition delay as the temperature increases. This phenomenon is well known for hydrocarbons with a sufficiently long carbon chain and has been described elsewhere.[19] It can be explained briefly by a transition from the well–known low–temperature branching, which relies on the subsequent reactivity of peroxyalkyl radicals $RO_2$ , to the more competitive but slower mechanism associated with intermediate temperatures. When the temperature increases because of the development of the exothermic cool flame, these $RO_2$ adducts become less and less stable, while at the same time the concentration of $HO_2$ radicals builds up. This explains the brutal diminution of the global reactivity that is associated with the extinction of the cool flame. The $HO_2$ radicals can react with hydrocarbon molecules to yield $H_2O_2$, which will in turn decompose into two OH radicals when the temperature is high enough. The squares represent autoignition, the circles plasma assisted ignition.

The ignition delay time is significantly shorter in the case of plasma assisted ignition than for autoignition, in the whole investigated temperature range. The plasma assisted ignition case shows no negative temperature dependence of the ignition delay with temperature. As it is known,[2,4,9] the action of nonequilibrium plasma on the hydrocarbon-oxygen mixture in the wide range of electric fields, E/N=100–300 Td, is the following: acceleration of electrons in the electric field leads to ionization, excitation of electronic levels of atoms and molecules and to dissociation. This process leads to an essential increase in the densities of O, H atoms, and $C_nH_{2n+1}$ radicals at the beginning of ignition, and to accumulation of intermediate components, like CO and HCHO, at the period of the ignition delay.[9] To explain the details of the chemical processes associated with the discharge in RCM conditions of high pressures, further experimental and theoretical investigations of both the discharge and modified combustion system should help explain these results.

## IV. Conclusions

The experimental study of parameters of nanosecond surface dielectric barrier (SDBD) discharge has been made in synthetic air for a pressure range 1–5 atm on the basis of the emission of molecular nitrogen. Electric fields were measured for positive and negative polarities of the discharge at pulse duration 20 ns and pulse amplitude 20–24 kV on the high voltage electrode. The main observations and conclusions from the comparison are the following: (i) no crucial dependence of electric field on the HV pulse front is observed; (ii) the peak value of the electric field decreases with pressure (from 1000 to 500 Td at the edge of the electrode for positive polarity of the pulse), while the second part remains practically the same, about 400–500 Td; (iii) for the negative polarity, E/N values are lower than for the positive polarity: for the second part of the signal the electric fields at the negative polarity are about 200 Td instead of 400–500 for the positive polarity. Although the values at negative polarity are lower, they are still too high to be explained by a streamer propagation theory without additional assumptions about the geometry of the discharge and the presence of a ultra-high electric field region between a streamer and a surface. The additional analysis of the obtained experimental data together with comprehensive numerical modeling is necessary to draw further conclusions about the electric field value in a surface DBD discharge. ICCD imaging of the discharge in argon and air confirms quasi–2D development of the discharge with simultaneous, within 2 ns, start of the streamers from a high-voltage electrode. Radial development of the discharge with a well–pronounced back wave is observed. Discharge structure depends upon the gas composition and voltage amplitude.

Experiments comparing autoignition and ignition by sliding nanosecond DBD discharge have been made in a Rapid Compression Machine (RCM). A few combustible mixtures, based on methane and n-butane, with stoichiometric ratios from 0.3 to 1, and dilution by Ar or N2 by 70-80%, were tested. The studied temperatures ranged from 665 K to 960 K, and the pressures were between 7.5 and 15 atm. It was shown that the action of the discharge leads to a significant decrease of the ignition delay in all the investigated conditions. Knocking reduction was observed consistently in some experimental conditions: The pressure increase for the plasma-assisted ignition cases in knocking-sensitive regimes was less sharp than for autoignition. In the case of a fuel whose ignition delay has a negative temperature dependence, the induction delay times in the presence of the discharge varied monotonously with the temperature. Further experimental and numerical work is planned to understand the interactions between the discharge and the complex thermokinetic interactions associated with the ignition.

## V. Acknowledgements

The authors are extremely thankful to Dr. Pascale Desgroux for her help in launching the Project, for her continuous interest to the subject and for the fruitful discussions concerning the obtained results. The authors are thankful to J. Guillon (LPP), and for Sebastien Batut (PC2A) for technical assistance. The work was partially supported by French National Agency, ANR (PLASMAFLAME Project, 2011 BS09 025 01), PICS-RFBR grant (5745–11.02.91063–a/5745) and EOARD AFOSR, grant FA8655–10–1–3018, RFBR project 10-01-00468-a. Work of S. Starikovskaia and S. Stepanyan was partially supported by PUF (Partner University Foundation). Project. the authors are thankful for Prof. Ju (Princeton University) and Dr. Popov (Moscow State Universiry) for fruitful discussions.

## References

[1]Starikovskaia S M 2006 Plasma assisted ignition and combustion J. Phys. D.: Appl. Phys. 39 R265-99; Starikovskaia S M and Starikovskii A Yu 2010 *Plasma assisted ignition and combustion Handbook of Combustion* **vol 5** New Technologies ed M Lackner et al (Weinheim: Wiley-VCH)

[2]Adamovich I V, Choi I, Jiang N, Kim J-H, Keshav S, Lempert W R, Mintusov E, Nishihara M, Samimy M and Uddi M 2009 Plasma assisted ignition and high-speed flow control: non-thermal and thermal effects *Plasma Sources Sci. Technol.* **18** 034018

[3]Starikovskiy A and Aleksandrov N 2011 Plasma-Assisted Ignition and Combustion Aeronautics and Astronautics, ed Max Mulder (Rijeka: InTech) pp 331-368

[4]Popov N A, Effect of nonequilibrium excitation on the ignition of combustion mixtures. *Proc. of 43rd AIAA Plasmadynamics and Laser Conference*, 25-28 June 2012, New Orleans, USA.

[5]Kof L M, Starikovskii A Yu, Abstract of Papers, *26th Int. Symp. on Combustion*, Napoli, 1996, p. 406.

[6]Bozhenkov S A, Starikovskaia S M, Starikovskii A Yu 2002 Nanosecond gas discharge ignition of $H_2$- and $CH_4$ - containing mixtures *Comb. and Flame* **133** 133-146

[7]Starikovskaia S M, Kukaev E N, Kuksin A Yu, Nudnova M M, Starikovskii A Yu 2004 Analysis of the spatial uniformity of the combustion of a gaseous mixture initiated by a nanosecond discharge *Comb. and Flame* **139** 177-187

[8]Kosarev I N, Aleksandrov N L, Kindysheva S V, Starikovskaia S M, Starikovskii A Yu 2008 Kinetics of ignition of saturated hydrocarbons by nonequilibrium plasma: $CH_4$-containing mixtures *Comb. and Flame* **154** 569-586

[9]Kosarev I N, Aleksandrov N L, Kindysheva S V, Starikovskaia S M, Starikovskii A Yu 2009 Kinetics of ignition of saturated hydrocarbons by nonequilibrium plasma: $C_2H_6$- to $C_5H_{12}$-containing mixtures *Comb. and Flame* **156** 221-223

[10]Starikovskaya S M, Aleksandrov N L, Kosarev I N, Kindysheva S V, Starikovskii A Yu, 2009 Ignition with low-temperature plasma: kinetic mechanism and experimental verification, Invited Review Paper *High Energy Chemistry* **43/3**, 213-218

[11]Pancheshnyi S V, Lacoste D A, Bourdon A, Laux C O 2006 Ignition of propane–air mixtures by a repetitively pulsed nanosecond discharge *IEEE Trans. on Plasma Science* **34 (6)** 2478—2487

[12]Bentaleb S, Tardiveau P, Jorand F, Jeanney P, Magne L, Pasquiers S 2011 Ignition of $N_2/O_2/C_3H_8$ mixtures by a single nanosecond pulsed discharge at atmospheric pressure *Proc. of International Conference on Plasma Physics (ISPC)* Philadelphia, USA, 4—9 July 2011

[13]Markus D, Hallermann A, Langer T, Paul M, Lienesch F 2011 Experimental investigation of the ignition by repetitive streamer discharges *42nd AIAA Plasmadynamics and Lasers Conference*, 27–30 June 2011, Honolulu, Hawaii, AIAA 2011—3451

[14]Singleton D, Pendleton S J, Gundersen M A 2011 The role of non–thermal transient plasma for enhanced flame ignition in $C_2H_4$—air *J. Phys. D: Appl. Phys.* **44** 022001 (6pp)

[15]Kosarev I N, Khorunzhenko V I, Mintoussov E I, Sagulenko P N, Popov N A, Starikovskaia S M, 2012 A nanosecond surface dielectric barrier discharge at elevated pressures: time-resolved electric field and efficiency of initiation of combustion *Plasma Sources Sci. Technol.* **21** (2012) 045012 (15pp)

[16]Opaits D F, Roupassov D V, Saddoughi S G, Starikovskaia S M, Zavialov I N and Starikovskii A Yu, 2005 Plasma control

of boundary layer using low-temperature non-equilibrium plasma of gas discharge, *Proc. of 43rd AIAA Aerospace Sciences Meeting and Exhibit* (Reno, Nevada, USA, 2005) Paper AIAA 2005-1180

[17]Starikovskii A Yu, Nikipelov A A, Nudnova M M, Roupassov D V, 2009 SDBD plasma actuator with nanosecond pulse-periodic discharge, *Plasma Sources Sci. Technol.* **18** 034015 (17pp)

[18]Little J, Takashima K, Nishihara M, Adamovich I, Samimy M, 2012 Separation control with nanosecond pulse driven dielectric barrier discharge plasma actuators *AIAA Journal* **50** pp. 350-365

[19]Vanhove G, Petit G, Minetti R, 2006 Experimental study of the kinetic interactions in the low–temperature autoignition of hydrocarbon binary mixtures and a surrogate fuel, *Combustion and Flame* **145(3)** 521—532

[20]Tanaka S, Ayala F, Keck J C, 2003 A reduced chemical kinetic model for HCCI combustion of primary reference fuels in a rapid compression machine, *Combustion and Flame* **133(4)** 467—481

[21]Goldsborough S S, Banyon C, Mittal G, 2012 A computationally efficient, physics–based model for simulating heat loss during compression and the delay period in RCM experiments, *Combustion and Flame* **159(12)** 3476—3492

[22]Mittal G, Raju M P, Sung C–J, 2010 CFD modeling of two-stage ignition in a rapid compression machine: Assessment of zero–dimensional approach *Combustion and Flame* **157(7)** 1316—1324

[23]Starikovskiy A, Rakitin A, Correale G, Nikipelov A, Urushihara T, Shiraishi T, 2012, Ignition of hydrocarbon-air mixtures by nonequilibrium plasma at elevated pressures up to 40 bar *Proc. of 50th AIAA Aerospace Sciences Meeting Including the New Horizons Forum and Aerospace Exposition* 9 - 12 Jan 2012, Nashville, USA.

[24]Pancheshnyi S V, Starikovskaia S M and Starikovskii A Yu 1998 Measurements of rate constants of the $N_2$ ($C^3\Pi_u$, $v' = 0$), and $N_2^+$ ($B^2\Sigma_u^+$, $v' = 0$) deactivation by $N_2$, $O_2$, $H_2$, CO and $H_2O$ molecules in afterglow of the nanosecond discharge *Chemical Physics Letters* **29** 523—7

[25]Paris P, Aints M, Valk F, Plank T, Haljaste A, Kozlov K V, and Wagner H–E 2005 Intensity ratio of spectral bands of nitrogen as a measure of electric field strength in plasmas*J. Phys. D: Appl. Phys.* **38** 3894

[26]Paris P, Aints M and Valk F, 2009 Collisional quenching rates of $N_2^+(B^2\Sigma_g^+, v = 0)$, *Book of contributed papers of 17th Symposium on Application of Plasma Processes and Visegrad Workshop on Research of Plasma Physics* Liptovsky Jan, Slovakia, 17–22 January 2009, pp. 227—8

[27]Mintoussov E I , Pendleton S J, Gerbault F G, Popov N A, Starikovskaia S M, 2011 Fast gas heating in nitrogen-oxygen discharge plasma: II. Energy exchange in the afterglow of a volume nanosecond discharge at moderate pressures *J. Phys. D: Appl. Phys.* **44** 285202 (13pp)

[28]Lee D, Hochgreb S, 1998 Rapid Compression Machines: Heat Transfer and Suppression of Corner Vortex *Combustion and Flame* **114(3–4)** 531—545

[29]Soloviev V R, Krivtsov V M, Konchakov A M and Malmuth N D 2008 Surface barrier discharge simulation in air for constant applied voltage it AIAA Meeting (Reno, NV, January 2008) AIAA 2008-1378

[30]Soloviev V R, Krivtsov V M, Surface barrier discharge modelling for aerodynamic applications 2009 *J. Phys. D: Appl. Phys.* **42** 125208 (13pp) [crochet] M. Crochet, R. Minetti, M. Ribaucour, G. Vanhove, A detailed experimental study of n-propylcyclohexane autoignition in lean conditions, Combustion and Flame, Volume 157, Issue 11, November 2010, Pages 2078-2085

[31]Takashima (Udagawa) K, Zuzeek Y, Lempert W R, and Adamovich I V, 2011 Characterization of surface dielectric barrier discharge plasma sustained by repetitive nanosecond pulses *Plasma Sources Science and Technology* **20** 055009